

Thermal stress simulation of ultrafine plate-fin structures using a homogenization theory

Hiromu Kobori¹, *Tetsuya Matsuda¹, and Masahiro Arai²

¹ Department of Engineering Mechanics and Energy, University of Tsukuba
1-1-1 Tennodai, Tsukuba, 305-8573, Japan.

² Department of Mechanical Systems Engineering, Shinshu University
4-17-1 Wakasato, Nagano, 380-8553, Japan

*Corresponding author: matsuda@kz.tsukuba.ac.jp

Key Words: *Homogenization, Ultrafine plate-fin structure, Thermal stress, Thermal expansion*

Abstract

In this work, the thermal stress in ultrafine plate-fin structures made of a Ni-based alloy subjected to a macroscopic temperature increment is simulated macroscopically and microscopically, using a homogenization theory for thermoelastoviscoplasticity. For this purpose, the homogenization theory for thermoelastoviscoplasticity is constructed by introducing the effects of thermal expansion into the homogenization theory for time-dependent materials. The present theory is then applied to the thermal stress simulation of ultrafine plate-fin structures, in which three cases of macroscopic temperature rates are considered. The results show that the higher the macroscopic temperature rate is, the higher the thermal stress is. Moreover, it is shown that the stress concentration occurs at joint regions between plates and brazing parts, and at some parts of fins, indicating the importance of thermal stress analysis of ultrafine plate-fin structures.

Introduction

High temperature gas-cooled reactor gas-turbine (HTGR-GT) systems have been regarded as some of the most promising power generating systems. The HTGR produces much higher outlet temperature than conventional reactors. Using the thermal energy, the total efficiency of the systems can be increased (Po-Jui et al, 2008). In the systems, helium is employed as a working fluid, and can reach 850~950°C in heat exchangers. In such a high temperature condition, the heat exchangers encounter severer thermal loads. Especially when a reactor scram happens, they may become even severer due to the steep change of helium temperature. In fact, a lot of studies as to structural integrity of heat exchangers in scram events have been performed at the high temperature engineering test reactor (HTTR) built in Japan, which is an experimental reactor of HTGR (Tachibana et al, 2003).

Ultrafine plate-fin structures for heat exchangers manufactured by stacking thin metallic plates and fins alternately (Fig. 1) offer high heat-exchange efficiency, because their small structures provide large heat-transfer areas. Thus, they are expected to be used in the heat exchangers of HTGR-GT systems (Kawashima et al, 2007). It is therefore important to estimate high temperature structural

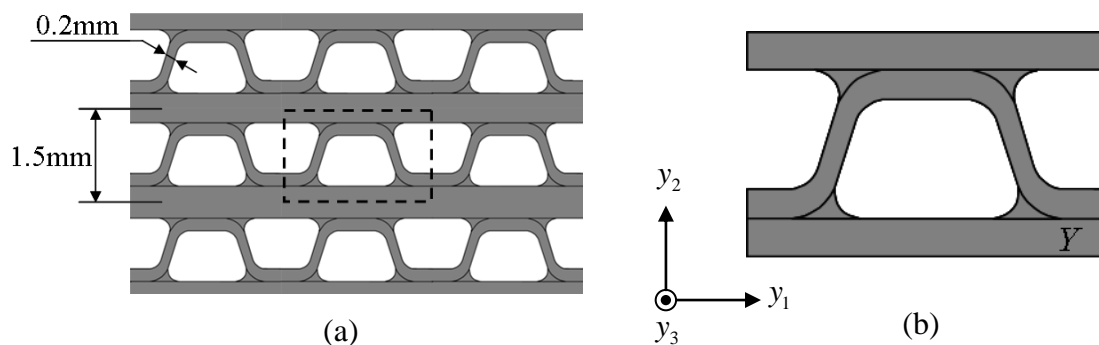


Figure 1. Ultrafine plate-fin structures: (a) whole structure. (b) its unit cell *Y*

integrity of ultrafine plate-fin structures. In particular, analyzing their inelastic thermal behavior in scram events is indispensable for designing heat exchangers.

In general, ultrafine plate-fin structures have such complicated microstructures that it is difficult to analyze their mechanical properties, although there have been some reports on elastic/inelastic analysis of plate-fin structures. For example, Tsuda et al. (2010) analyzed the macroscopic elastic-viscoplastic behavior of ultrafine plate-fin structures based on a homogenization technique (Sanchez-Palencia, 1980) using the FEM, and succeeded in developing a macroscopic constitutive model which can reproduce the homogenized elastic-viscoplastic behavior of plate-fin structures. In their study, however, they did not take thermal stress into consideration. On the other hand, Shabana and Noda. (2008) analyzed the elastic thermal stress of unidirectional fiber-reinforced plastic composites using a homogenization theory for thermoelasticity, and showed the accuracy of the theory by comparing the results with experimental ones. However, elastic thermal stress analysis is not sufficient for ultrafine plate-fin structures because inelastic thermal stress can occur in them during scram events.

In the present study, therefore, the thermal stress in ultrafine plate-fin structures subjected to a macroscopic temperature increment is simulated macroscopically and microscopically, using a homogenization theory for thermoelastoviscoplasticity. For this purpose, the homogenization theory for thermoelastoviscoplasticity is constructed by introducing the effects of thermal expansion into the homogenization theory for time-dependent materials (Ohno et al., 2000). The present theory is then applied to the thermal stress simulation of ultrafine plate-fin structures, in which three cases of macroscopic temperature rates are considered.

Homogenization Theory for thermoelastoviscoplasticity

In this section, the homogenization theory for thermoelastoviscoplasticity is constructed by introducing the effects of thermal expansion into the homogenization theory for time-dependent materials (Ohno et al., 2000).

Let us consider an ultrafine plate-fin structures shown in Fig. 1(a), its unit cell having been defined as Y (Fig. 1(b)). For this Y , the Cartesian coordinates y_i ($i=1, 2, 3$) are defined, and microscopic stress and strain fields are denoted by σ_{ij} and ε_{ij} , respectively. Then, the equilibrium of σ_{ij} can be expressed in a rate form as

$$\dot{\sigma}_{ij,j} = 0, \quad (1)$$

where $(\dot{\cdot})$ and $(\cdot)_{,j}$ indicate the differentiation regarding t and y_j , respectively. The base material of the plate-fin structure is assumed to exhibit linear elasticity and non-linear viscoplasticity as characterized by

$$\dot{\sigma}_{ij} = c_{ijkl} (\dot{\varepsilon}_{kl} - \beta_{kl} - \Delta\dot{T}\alpha_{kl}), \quad (2)$$

where c_{ijkl} , β_{kl} , $\Delta\dot{T}$ and α_{kl} stand for the elastic stiffness, viscoplastic strain rate, macroscopic temperature increment and the coefficient of thermal expansion of the base material, respectively.

Let $v_i(\mathbf{y}, t)$ be an arbitrary variation of the perturbed velocity field defined in Y at t . Then, the integration by parts and the divergence theorem allow Eq. (1) to be transformed to

$$\int_Y \dot{\sigma}_{ij} v_{i,j} dY - \int_{\Gamma} \dot{\sigma}_{ij} n_j v_i d\Gamma = 0, \quad (3)$$

where Γ denotes the boundary of Y , and n_j indicates the unit vector outward normal to Γ . In Eq. (3), the second term of the left-hand side, i.e. the boundary integral term, vanishes because of the following reason: on the boundaries, $\dot{\sigma}_{ij}$ and v_i satisfy the Y -periodicity, while n_i takes an opposite direction on an opposite boundary facet. Thus, the boundary integral term becomes zero. Consequently, Eq. (3) results in

$$\int_Y \dot{\sigma}_{ij} v_{i,j} dY = 0. \quad (4)$$

The above equation and Eq. (2) derive

$$\int_Y c_{ijpq} \dot{u}_{p,q}^{\#} v_{i,j} dY = -\dot{E}_{kl} \int_Y c_{ijkl} v_{i,j} dY + \int_Y c_{ijkl} \beta_{kl} v_{i,j} dY + \Delta\dot{T} \int_Y c_{ijkl} \alpha_{kl} v_{i,j} dY, \quad (5)$$

where $u_i^\#$ and \dot{E}_{ij} denote the perturbed displacement and macroscopic strain, respectively. They are related as follows:

$$\dot{u}_i^\# = \chi_i^{kl} \dot{E}_{kl} + \varphi_i + \Delta T \dot{\psi}_i. \quad (6)$$

The functions χ_i^{kl} , φ_i and ψ_i in the above equation are called the characteristic functions, and can be obtained by solving the following boundary value problems:

$$\int_Y c_{ijpq} \chi_{p,q}^{kl} v_{i,j} dY = - \int_Y c_{ijkl} v_{i,j} dY, \quad (7)$$

$$\int_Y c_{ijpq} \varphi_{p,q} v_{i,j} dY = \int_Y c_{ijkl} \beta_{kl} v_{i,j} dY, \quad (8)$$

$$\int_Y c_{ijpq} \psi_{p,q} v_{i,j} dY = \int_Y c_{ijkl} \alpha_{kl} v_{i,j} dY. \quad (9)$$

The microscopic relation and the macroscopic constitutive equation are as follows:

$$\dot{\sigma}_{ij} = c_{ijpq} (\delta_{pk} \delta_{ql} + \chi_{p,q}^{kl}) \dot{E}_{kl} - c_{ijkl} (\beta_{kl} - \varphi_{k,l}) - \Delta T \dot{c}_{ijkl} (\alpha_{kl} - \psi_{k,l}), \quad (10)$$

$$\dot{\Sigma}_{ij} = \langle c_{ijpq} (\delta_{pk} \delta_{ql} + \chi_{p,q}^{kl}) \rangle \dot{E}_{kl} - \langle c_{ijkl} (\beta_{kl} - \varphi_{k,l}) \rangle - \Delta T \langle c_{ijkl} (\alpha_{kl} - \psi_{k,l}) \rangle, \quad (11)$$

where δ_{ij} indicates Kronecker's delta, and

$$\langle \# \rangle = \frac{1}{|Y|} \int_Y \# dY. \quad (12)$$

Here, $\langle \rangle$ designates the volume average in Y , and $|Y|$ signifies the volume of Y .

Analysis Conditions

In the present analysis, macroscopic stress-temperature relations and microscopic thermal stress of ultrafine plate-fin structures were analyzed using the theory mentioned above. Table 1 shows the temperature conditions. Assuming that a reactor scram occurs, the macroscopic temperature change from 950°C to 360°C was given to the plate-fin structures. Three cases of macroscopic temperature rate, i.e. $\Delta T = -0.05$, -0.25 and -0.5°C/s , were considered. These temperature conditions were determined by referring to the data obtained by a reactor scram experiment done at HTTR. The macroscopic strain was set to zero ($\dot{E}_{ij} = 0$).

A unit cell Y was defined and divided into four-node isoparametric elements as illustrated in Fig. 2. This Y was two-dimensional rather than three-dimensional, and the generalized plane strain condition was assumed, because the plate-fin structures were assumed to have uniform and infinite

Table 1. Temperature conditions

Macroscopic temperature increment	$\Delta T [^\circ\text{C}]$	-590
		1. -0.05
Macroscopic temperature increment per second	$\Delta \dot{T} [^\circ\text{C/s}]$	2. -0.25
		3. -0.5

Table 2. Material properties(HastelloyX)

Poisson's ratio	ν	0.32
Reference strain rate	$\varepsilon_0 [s^{-1}]$	10^{-3}
Stress power index	n	$-0.0295T + 33.075$
Young's modulus	$E [\text{GPa}]$	$-0.0684T + 212.22$
Coefficient of thermal expansion	$\alpha [10^{-6}/\text{K}]$	$0.0031T + 13.548$

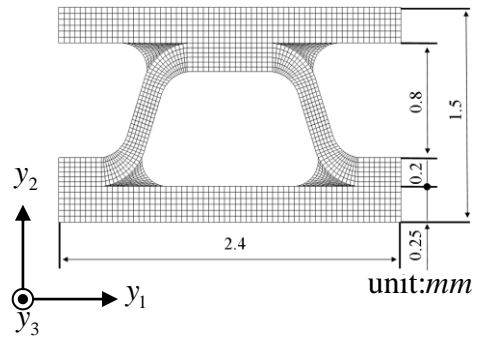


Figure 2. Unit cell Y and its finite element mesh

material distribution in the y_3 -direction. A base metal for the plate-fin structures was Hastelloy X, which was a Ni-based alloy with excellent heat resistance. The Hastelloy X was regarded as an isotropic elastic-viscoplastic material characterized by the following constitutive equation:

$$\dot{\epsilon}_{ij} = \frac{1+\nu}{E} \dot{\sigma}_{ij} - \frac{\nu}{E} \dot{\sigma}_{kk} \delta_{ij} + \frac{3}{2} \dot{\epsilon}_0^p \left(\frac{\sigma_{eq}}{\sigma_0} \right)^{n-1} \frac{s_{ij}}{\sigma_0}, \quad (13)$$

where, E and ν indicate elastic constants, $\dot{\epsilon}_0$ and σ_0 represent reference strain rate and reference stress, respectively, n is a material parameter of viscoplasticity, s_{ij} stands for the deviatoric part of σ_{ij} , and $\sigma_{eq} = [(3/2)s_{ij}s_{ij}]^{1/2}$. Here, n , E and α were the parameters dependent on the current temperature T . Material constants used are listed in Table 2.

Results

Figures 3 (a) and (b) respectively show the macroscopic stress-temperature relations of the plate-fin structures at $\Delta T = -0.05^\circ\text{C/s}$ and -0.5°C/s . Due to the lack of space, the stress-temperature curves when $\Delta T = -0.25^\circ\text{C/s}$ are omitted. From Figs. 3(a) and (b), stress-temperature relations in the y_1 , y_2 and y_3 directions are markedly different from one another, indicating the thermoelastoviscoplastic anisotropy resulting from the complicated microstructures of plate-fin structures. Moreover, it can be seen that, comparing Fig. 3(a) with (b), the maximum tensile stress of Fig. 3(b) is higher than that of (a) on each direction: the maximum increase is about 10%. This means that the higher the macroscopic temperature rate is, the higher the macroscopic thermal stress is. Incidentally, macroscopic shear stress did not occur.

Next, Figs. 4(a) and (b) show the deformed unit cells and the microscopic Mises's equivalent stress distributions at 360°C when $\Delta T = -0.05^\circ\text{C/s}$ and -0.5°C/s , respectively. The displacement is magnified five times. As seen from these figures, high stress concentration occurs in the middle of the fins, and moreover, the stress concentration also occurs at joint regions between plates and brazing parts. Comparing Fig. 4(a) with (b), the maximum tensile stress of Fig. 4(b) is about 10%

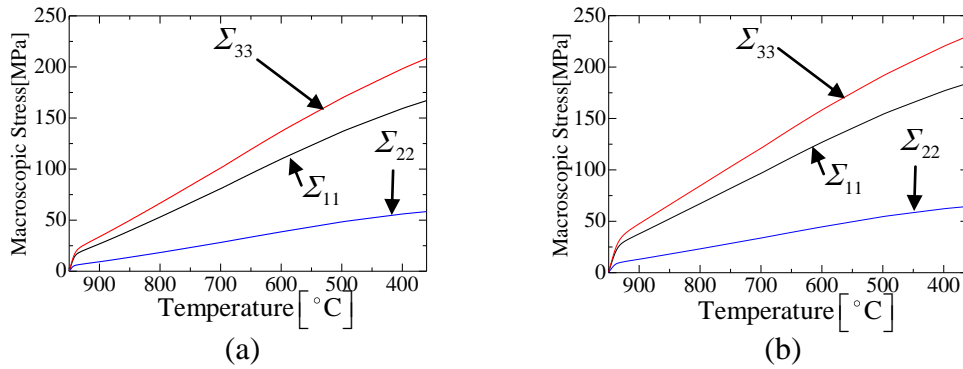


Figure 3. Macroscopic Stress-Temperature curves on different macroscopic temperature increment per second; (a) -0.05°C/s , (b) -0.5°C/s

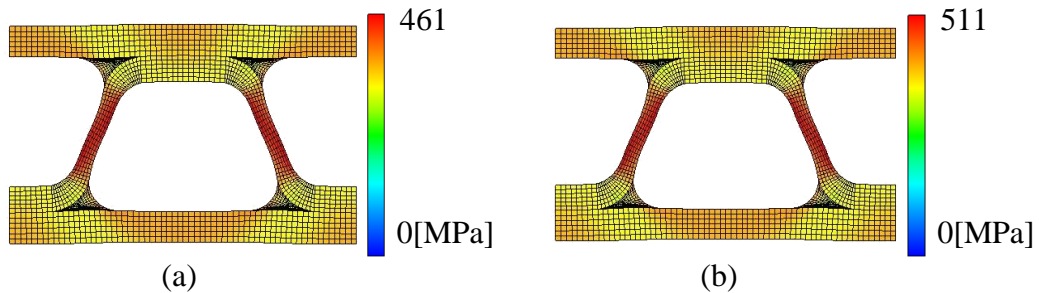


Figure 4. Microscopic Mises's equivalent stress distribution at 360°C on different macroscopic temperature increment; (a) -0.05°C/s , (b) -0.5°C/s

higher than that of (a). This indicates that the higher the macroscopic temperature rate is, the higher the microscopic thermal stress is, too.

Conclusions

In this study, the homogenization theory for thermoelastoviscoplasticity was proposed and the thermal stress simulation of ultrafine plate-fin structures was performed. In the analysis, the plate-fin structures experienced macroscopic temperature change from 950°C to 360°C assuming a reactor scram. Three patterns of macroscopic temperature rates are considered. The results are as follows.

- (1) The stress-temperature relations of ultrafine plate-fin structures in the y_1 , y_2 and y_3 directions are markedly different from one another, indicating the thermoelastoviscoplastic anisotropy of plate-fin structures.
- (2) The stress concentration occurs at joint regions between plates and brazing parts, and at some parts of fins.
- (3) The higher the macroscopic temperature rate is, the higher both the macroscopic and microscopic thermal stresses are.

These results show that high thermal stress can occur in the case of the scram events, indicating the importance of inelastic thermal stress analysis of ultrafine plate-fin structures.

References

- Kawashima, F., Igari, T., Miyoshi, Y., Kamito, Y. and Tanihira, M. (2007), High temperature strength and inelastic behavior of plate-fin structures for HTGR. *Nuclear Engineering and Design*, 237, pp. 591–599.
- Ohno, N., Wu, X. and Matsuda, T. (2000), Homogenized properties of elastic-viscoplastic composites with periodic internal structures. *International Journal of Mechanical Sciences*, 42, pp. 1519-1536.
- Po-Jui, L., Tzu-Chen, H., Bau-Shei, P., Jaw-Ren, L., Ching-Chang, C. and Ge-Ping, Y. (2012), A thermodynamic analysis of high temperature gas-cooled reactors for optimal waste heat recovery and hydrogen production. *Applied Energy*, pp. 183-191.
- Sanchez-Palencia, E. (1980), Non-homogeneous Media and Vibration Theory. Lecture Notes in Physics 127, Springer-Verlag.
- Shabana, Y. M. and Noda, N. (2008), *International Journal of Solids and Structures*, 45, pp. 3494-3506.
- Tachibana, Y., Nakagawa, S., Takeda, T., Saikusa, A., Furusawa, T., Takamatsu, K., Sawa, K. and Iyoku, T. (2003), Plan for first phase of safety demonstration tests of the High Temperature Engineering Test Reactor (HTTR). *Nuclear Engineering and Design*, pp. 179-197
- Tsuda, M., Takemura, E., Asada, T., Ohno, N. and Igari, T. (2010), Homogenized elastic-viscoplastic behavior of plate-fin structures at high temperatures: Numerical analysis and macroscopic constitutive modeling. *International Journal of Mechanical Sciences*, 52, pp. 648-656.